

Characterizing the detection system nonlinearity, internal inelastic background, and transmission function of an electron spectrometer for use in x-ray photoelectron spectroscopy

R. C. Wicks and N. J. C. Ingle

Advanced Materials and Process Engineering Laboratory, University of British Columbia, 2355 East Mall, Vancouver, British Columbia V6T 1Z4, Canada

(Received 27 February 2009; accepted 20 April 2009; published online 11 May 2009)

We present a method for removing spectrometer specific contributions to x-ray photoelectron spectroscopy data. We consider the degree of linearity of the detection system, the strength of the internal analyzer inelastic background, and finally determine the spectrometer's transmission function. The procedures presented here are performed on a SPECS Phoibos 150 hemispherical analyzer with a two-dimensional detection system, but are applicable to a wide variety of different electron spectrometers. The spectrometer's detection system is found to deviate from linear behavior by a few percent over the whole intensity range studied. The size of the analyzer internal inelastic scattering has been measured, and we find that it can normally be neglected at large pass energies or high kinetic energies for most types of analysis (contributing less than 1% at 100 eV pass energy). Finally, we measure the transmission function of the analyzer and lens system for a variety of different settings with the preceding corrections applied, and find that the form of the transmission function is dependent on small changes in the system's settings. © 2009 American Institute of Physics. [DOI: 10.1063/1.3131631]

I. INTRODUCTION

X-ray photoelectron spectroscopy (XPS) is a powerful tool for studying the chemical properties of the surface of materials. With it, we can learn about a material's electronic structure, chemical composition, surface contaminants, and oxidation state by measuring a combination of core level peak positions for chemical state information and relative peak areas for quantitative analysis. This requires a spectrometer that is well calibrated not just for energy position, but also absolute intensity. From a film grower's perspective, XPS is an ideal tool to characterize the properties of thin-film based materials because it is surface sensitive and non-destructive. Perhaps most important, XPS can be performed *in situ*, allowing the characterization of sensitive samples which must be handled completely in vacuum to prevent damage or contamination. For instance, films of transition metal or rare-earth oxides may not maintain their as-grown oxidation state when exposed to atmosphere. XPS measurements can even be performed at midgrowth, which is important for the characterization of thin-film heterostructures.

At the heart of any XPS measurement is an electron spectrometer. The most common electron spectrometer in use today is the hemispherical capacitor analyzer, also called the concentric hemisphere analyzer, shown schematically in Fig. 1. These spectrometers consist of a lens system which focuses and slows down the incoming electrons, a hemispherical capacitor analyzer that discriminates the electrons as a function of their kinetic energy, and a detection system that counts these discriminated electrons. The spectrometer has a large effect on the data that are collected. This is most often discussed in terms of a transmission function $T(E_k, E_p)$,¹⁻¹⁰

which describes the fraction of the total number of photoelectrons which are detected after being photoemitted from a sample with kinetic energy E_k and which then travel through the hemispheres with energy E_p (the so-called pass energy, to which the electrons have been decelerated by the analyzer lens system). Once the transmission function has been experimentally determined, it can be divided out from the measured spectra.

However, besides the transmission function, there are other ways spectrometers can affect XPS data; these include the sample-analyzer-photon source geometry, internal analyzer inelastic scattering, and detector nonlinearities. Weng *et al.*^{9,10} have compared the effectiveness of several methods for measuring the transmission functions for both an older model spectrometer as well as a more modern one with a two-dimensional detection system. They show that at any method of measuring the transmission function fails if there are unaccounted for nonlinearities in the detection system. Mannella *et al.*¹¹ measured the detector nonlinearity for a spectrometer with a two-dimensional detection system and find deviations from linear behavior as large as 40%. Detector nonlinearity is a function of the flux incident on the detector, and it cannot be divided out of the spectrum in the same way the transmission function can be. The internal analyzer inelastic background has also been studied by several authors¹²⁻¹⁴ and was shown to provide an additive contribution to the spectrum, which can be significant for certain choices of experimental parameters such as the pass energy. Since these two effects can both lead to E_k - and E_p -dependent contributions to the photoemission intensity

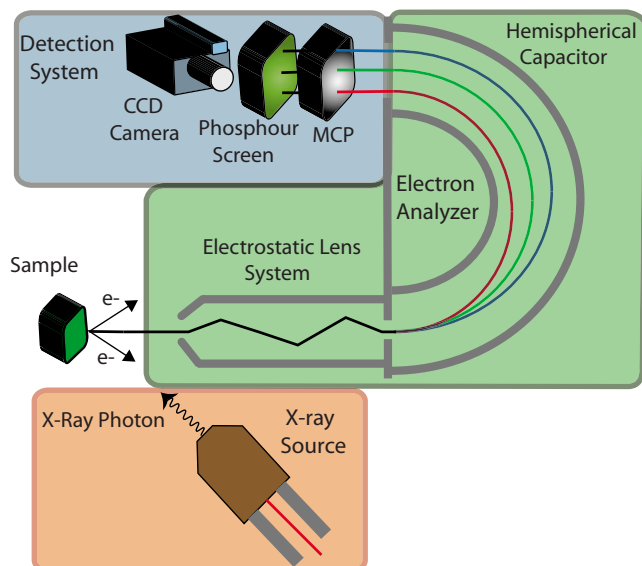


FIG. 1. (Color online) A diagram of the experimental setup of an XPS measurement. Electrons are photoexcited by an x-ray source, and those with sufficient kinetic energy are collected by the electrostatic lens. The lens focuses the electrons on the entrance slit of the hemispherical capacitor. The potential between the two concentric hemispheres in the capacitor produces an electrostatic field which discriminates the electrons as a function of kinetic energy as they pass between the hemispheres. A multichannel plate amplifies increases the electron signal before it impinges on a phosphor screen and is measured by a CCD camera.

and cannot be simply divided out from the spectrum, they both must be addressed prior to the characterization of the transmission function.

The goal of this work is to measure the probability of an electron getting through the electron analyzer and being measured by the detection system as a function of the spectrometer settings, electron kinetic energy and intensity. This is a critical first step in performing quantitative analysis of XPS data using peak area or peak height analysis. Furthermore, if one wants to apply background subtraction based on physical arguments, such as the Tougaard background, the response of the spectrometer must be corrected.⁶

In this paper, we present a method in determining and removing the most important spectrometer specific contributions from an XPS spectrum. We deal with the various contributions to the final spectrum in the reverse order in which they are applied to the signal as it moves through the spectrometer. We first investigate the response of the detection system to applied flux. Second, we measure the internal analyzer inelastic background. Finally, after taking into account both of these effects, we determine the transmission function of the analyzer and lens system. We find that the transmission function for this spectrometer is strongly affected by changes in the lens mode, iris setting, and source spot size. This highlights the importance of measuring the transmission function in the exact configuration in which the spectrometer will be used when performing XPS measurements. We also find that the method used here to remove the transmission function can indicate or exclude the presence of other unaccounted for E_k - and E_p -dependent spectrometer contributions to XPS data.

II. EXPERIMENTAL DETAILS

We use a Phoibos 150 hemispherical electron analyzer produced by SPECS GmbH. This spectrometer relies on a multielement lens system to provide different types of imaging through a variety of lens modes. A schematic of the analyzer and detection system is shown in Fig. 1. There is an iris on the front of the lens system, which is used to define the sharpness of the acceptance area of the spectrometer. In this work, the iris is kept in the fully open position, except when noted. The spectrometer's detection system consists of a multichannel plate/phosphor screen and a charge-coupled device (CCD) camera from PCO (PixelFly) to record the two-dimensional spectrum. This spectrometer does not have a mesh between the analyzer and the detection system to electrically separate them. A one-dimensional spectrum is obtained by integrating over the direction perpendicular to the energy dispersion to produce a set of data similar to that which would be measured by a series of channeltron detectors.

The medium magnification and medium area lens modes are appropriate for general purpose XPS and will be used exclusively for this work. The medium magnification mode magnifies a small portion of the sample, and this magnified area is defined by voltages in the lens system. The medium area mode has a higher transmission than the medium magnification mode, and the sharpness of the acceptance area is defined entirely by the iris.

XPS spectra from *in situ* grown amorphous Au films are used to determine the detector nonlinearity, internal analyzer inelastic scattering, and transmission function. Base pressure in the analysis chamber was 10^{-9} mbar, and in all of our measurements, we observed no sample aging with our metallic samples. The x-ray source is an unmonochromated dual anode SPECS XR-50; Al $K\alpha$ radiation is used to determine the detector nonlinearity and Mg $K\alpha$ radiation is used to measure the transmission function from XPS data. All spectra are measured at normal incidence to the sample. The x-ray source, sample, and analyzer angle is fixed at the standard value of 54.7° . The remainder of the transmission function data is taken using an electron gun as the source (SPECS EQ 22) and measuring the electrons reflected of the Au sample surface.

III. LINEARITY

To measure the detector nonlinearity, we would like to expose the two-dimensional detection system to a wide range of known electron fluxes and measure the detector response. The ideal measurement entails exposing the detection system to a source of electrons which produces a uniform distribution of counts over the entire detector. However, the dual requirement of having a wide count rate range and a flat spectrum are difficult to realize in practice. The solution to this problem is to measure the most intense peaks in an XPS spectrum, which results in different electron fluxes on different regions of the detection system, as the total photocurrent is changed. Therefore, the response of the different regions of the detection system can be determined as a function of "spectral photocurrent," which is the fraction of the total

photocurrent at a certain kinetic energy. Since we use an x-ray source to generate our photocurrent, we must check that the latter is proportional to applied x-ray power and then quantify the relationship between them. To do this, an isolated sample was prepared and the total photocurrent was measured with an ammeter placed between sample and ground. The total photocurrent was found to respond slightly nonlinearly to the applied x-ray power. Therefore, we have used the measured photocurrents as the basis for all our later measurements, as opposed to applied x-ray power, so that when studying the detector's intensity response any deviation from a linear behavior can be ascribed to the detection system.

To measure the intensity response of the detection system, a spectrum of the Au 4*f* peaks is tracked as a function of total incident photocurrent. The Au 4*f* peak was used because it is a very intense peak that is also close to the Fermi edge, which reduces the background of inelastically scattered electrons. This means that the detector can be exposed to very low and very high count rates in the same exposure. The measurements are taken with a fixed retarding voltage and a pass energy of 100 eV. Using peaks at different kinetic energies did not change the response of the detection system, but reduced the range of counts we were able to sample. In Fig. 2(a) we present the XPS intensity versus spectral photocurrent measured at 1398 eV kinetic energy; this particular energy value, as shown in the inset of Fig. 2(b), corresponds to the maximum of the Au 4*f*_{7/2} peak and is where the highest detector count rate is observed. As indicated by the linear fit also shown in Fig. 2(a), the detector response is approximately linear over the whole accessible intensity range. However, the inspection of the percentage difference between data and linear fit [inset of Fig. 2(a)] provides evidence for some systematic deviations, particularly pronounced at low fluxes; while over most of the photocurrent range the difference is within $\pm 3\%$, at the lowest measured flux this is of about 6%. These deviations, although quantitatively small, might become significant when analyzing spectral features extending over a wide range of intensities. To characterize in more detail and remove this systematic deviation from purely linear behavior, in Fig. 2(b) we plot the XPS intensity versus photocurrent at 10 different kinetic energies along the Au 4*f* peak structure, together with the results of a third order polynomial fit of the whole data set. Note that this approach relies on the assumption that the lowest intensity data behave perfectly linearly; however, if the lowest fluxes exhibit deviations from linearity, this will lead to a substantial overestimation of the nonlinearity at large fluxes. Nevertheless, this particular choice of linear response allows us to compare our results to that of Mannella *et al.*¹¹ For our detection system, we find only a small deviation from linearity, one that is at least four times less strong than the result of Mannella *et al.*¹¹ We will use this data to correct the detection system nonlinearity before proceeding to the subsequent steps of our analysis of the spectrometer response.

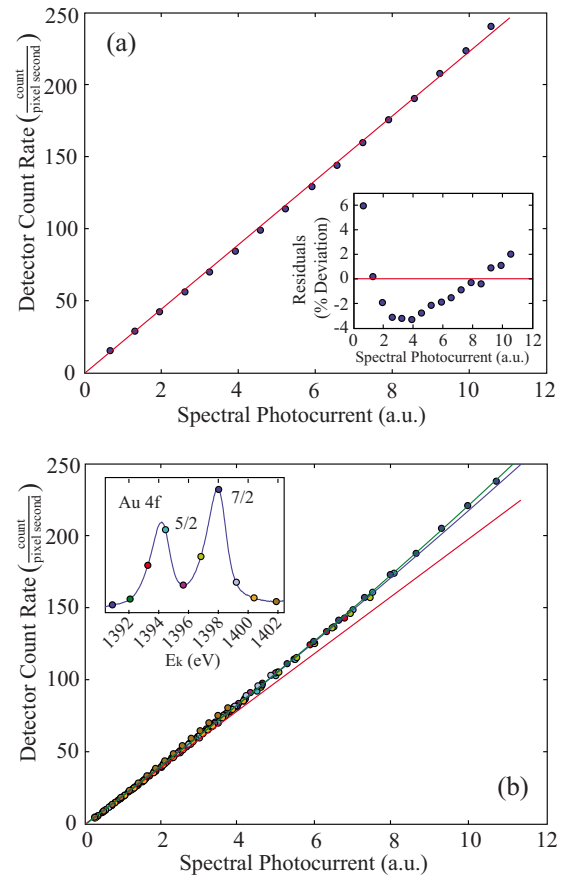


FIG. 2. (Color online) (a) Linear fit to the XPS intensity measured on a Au sample as a function of spectral photocurrent at 1398 eV kinetic energy [this corresponds to the maximum of the Au 4*f*_{7/2} peak as shown in the inset of (b)]; the percentage deviation from this linear fit is presented in the inset of (a). (b) XPS intensity vs spectral photocurrent at various kinetic energies along the Au 4*f* peak structure, as identified by the symbols (see inset). The solid lines represent the different contributions of a third order polynomial fit of the data (red: first order, blue: first and second orders, green: first, second, and third orders).

IV. INTERNAL ANALYZER INELASTIC SCATTERING

Next we will characterize the analyzer contribution to XPS spectra deriving from the internal inelastic scattering. The inelastic scattering taking place inside the analyzer complicates the analysis of signals at low pass energy and measurements of the transmission function. There can be many sources of internal inelastic scattering, including electrons scattered inside the lens, secondary electrons being liberated from the internal hemisphere by electrons below the pass energy, and electrons scattered from the hemisphere exit slit. The largest contribution, however, comes from electrons with energies higher than the pass energy that are scattered at the outer hemisphere.¹² Additionally, since our two-dimensional detection system incorporates a CCD camera, we will also have a constant background in our spectra associated with the camera dark count rate. This effect is unrelated to the analyzer internal inelastic scattering, but because the dark count rate has a similar effect on the spectra, we will deal with both problems at the same time. In this section we will only discuss the method to remove the analyzer internal inelastic background, but with the understand-

ing that this method will also remove the simpler flat background associated with the CCD camera dark count rate.

The method proposed by Battistoni *et al.*¹⁴ is used here to measure the internal analyzer inelastic background. It involves lowering the pass energy of the spectrometer (and consequently the transmission) so that any structure in the signal transmitted to the detection system drops below the level of the noise. The only contribution left in this case comes from the electrons that are inelastically scattered inside the analyzer.¹⁴ Since this background signal is independent of the transmission function, once it is measured it can be subtracted from other data sets acquired at different pass energies. This internal analyzer scattering is sample dependent, which has been previously verified by several authors,^{13,14} as well as dependent on the spectrometer setup and sample geometry/orientation; therefore it should be re-measured for every new experiment.

The contribution from the internal analyzer inelastic background for the SPECS Phoibos 150 hemispherical analyzer was measured by collecting spectra as the pass energy was lowered. We generally measured the same, peak-free spectra for all pass energies below 5 eV, suggesting that we were no longer measuring signals that originated from electrons passing through the lens with no inelastic collisions. Generally, the intensity of the spectra measured below 5 eV pass energy, the internal analyzer inelastic background, increases as the kinetic energy decreases. In everyday XPS analysis, with this particular spectrometer, the analyzer internal inelastic scattering will not be a major contributor to the overall signal. For spectra at 100 eV pass energy, its contribution is less than 1% of the total intensity integrated over kinetic energy, and can be neglected. It can, however, become very important for a spectrum taken at low pass energies; for instance, below 20 eV it contributes more than 20% of the integrated intensity and must be taken into account when measuring the transmission function.

V. TRANSMISSION FUNCTION

Once the internal inelastic background and detection system nonlinearities are corrected, the transmission function can be measured. We will discuss the transmission function for fixed analyzer transmission or constant analyzer energy mode, since it is the mode most often used in XPS. The photoemission intensity $I(E_k)$ can be written in a simplified form as¹⁵

$$I(E_k) = AB(E_k)T(E_k, E_p), \quad (1)$$

where A is a term that contains all of the sample and spectrometer factors that remain constant during a given experiment (e.g., geometry of the apparatus, acceptance area, photon flux, and sample chemical concentration), and $B(E_k)$ represents the sample kinetic-energy dependent contributions (mean free path of photoelectrons inside the sample and photoionization cross section). Finally, the transmission function of the electron analyzer and lens system $T(E_k, E_p)$ is the term in Eq. (1) we are most interested in determining.

Weng *et al.*^{9,10} have studied several different methods for measuring the transmission function of electron spectrometers. Of the variety of different methods that have been

proposed, we have chosen to use a method based on the work of Hemminger *et al.*⁸ This method entails choosing a functional form for the transmission function and using experimental data to fit this function (albeit in an unusual way). It offers advantages over other methods for a variety of reasons. First, it does not rely on *a priori* knowledge of the transmission function of another device or mode of operation of the same device. Second, the form of the transmission function can be derived from first principles by considering the transmission of electrons over the potential barrier created by the retarding field of the analyzer, as well as the trajectories of the electrons in this field. Third, and most importantly, the functional form of the transmission function allows one to mathematically isolate the kinetic energy and pass energy dependent transmission function from the kinetic energy dependent spectrum (this will be explained more below).

The form of the transmission function is presented in Eq. (2). If one ignores the exponent n , this equation has the quadratic dependence in pass energy and inverse dependence on kinetic energy that is expected for transmission through a retarding field.¹⁶ We must extend this equation so as to account for the deviations from the ideal behavior observed under realistic operational conditions; to do this, an exponent n is added to the E_p/E_k term (the inverse of the retard ratio term). n is itself a function of E_p/E_k , but no constraints are placed on its functional form so that the model has enough freedom to account for higher order terms of the inverse of the retard ratio as well as other deviations from the ideal behavior of the transmission function

$$T \propto E_p \left(\frac{E_p}{E_k} \right)^n. \quad (2)$$

To determine the transmission function, n must be mathematically separated from the A and $B(E_k)$ terms. This is done by substituting Eq. (2) into Eq. (1) and taking the natural logarithm of both sides, which yields

$$\ln \frac{I}{E_p} = \ln A + \ln B(E_k) + n \ln \frac{E_p}{E_k}. \quad (3)$$

As explained in more detail below, to experimentally find n we can now plot $\ln I/E_p$, where I is the measured photoemission intensity, versus $\ln E_p/E_k$ and then subtract the kinetic energy dependent offsets $\ln A + \ln B(E_k)$.

Applying the above method of extracting the transmission function involves measuring several spectra at different pass energies in the spectrometer mode of interest. Representative data taken in the medium area lens mode with a focused electron beam reflected off of a flat Au surface are shown in Fig. 3. The electron gun was set to 1600 eV kinetic energy; in the range of interest, and except for a small Auger structure at 250 eV, this produces a rather featureless spectrum of inelastically scattered electrons (decreasing in intensity for decreasing kinetic energy). Using the electron gun has the advantage of providing higher average intensity than is normally attainable in an XPS spectrum, allowing for faster data collection for an equivalent signal-to-noise value. The nonlinearity corrected data in Fig. 3 exhibit a pass energy dependent structure beyond a simple scaling of inten-

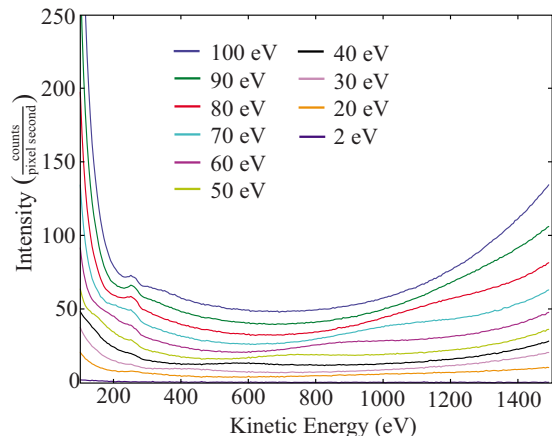


FIG. 3. (Color online) Electron gun spectra taken at different pass energies in medium area mode with an open iris, already corrected for intensity nonlinearity. The small structure at 250 eV kinetic energy is an Au Auger peak. The peak that moves as a function of kinetic energy is due to the transmission function. The 2 eV pass energy scan will be used to further correct for the internal analyzer inelastic background to obtain the processed data shown in Fig. 4.

sity, which moves to higher kinetic energy as the pass energy increases and stems from the pass energy dependence of the transmission function.

In order to extract n , once the data have been corrected for both nonlinearity and internal analyzer inelastic scattering, it is convenient to discuss intermediate data obtained from the measured photoemission intensity by plotting $\ln I/E_p$ versus $\ln E_p/E_k$. As emphasized by the black lines in the inset of Fig. 4, this yields one curve for each kinetic energy as a function of the nine measured pass energies ($E_p=2$ eV is only used for correcting the internal analyzer scattering), each curve with a different offset sample dependent offset $\ln A + \ln B(E_k)$. Most importantly, one should note that each of these fixed kinetic-energy curves represents a portion of the same $n=n(\ln E_p/E_k)$ function, albeit on a different range of $\ln E_p/E_k$ and with a different offset. To ex-

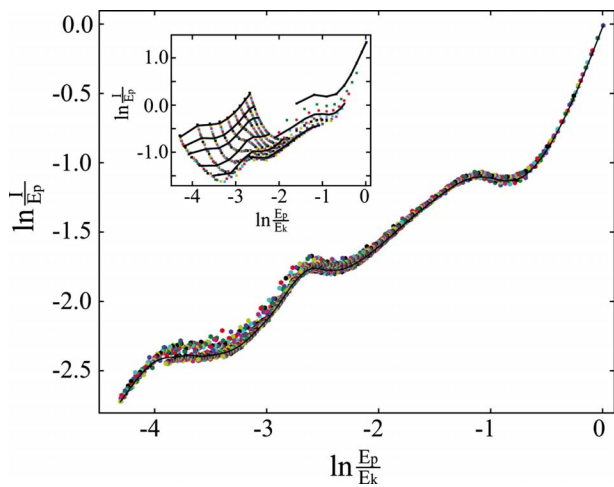


FIG. 4. (Color online) Intermediate transmission function data for medium area mode including the pass energy dependence of the sensitivity of the detection system. The detection system nonlinearity, internal analyzer inelastic scattering, and $\ln A + \ln B(E_k)$ offset have been removed. The inset shows the data before offset removal; each black line identifies a data set characterized by fixed kinetic energy and varying pass energy.

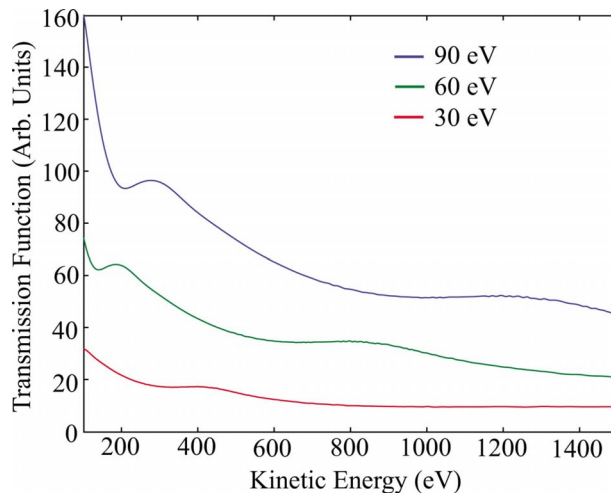


FIG. 5. (Color online) Experimentally determined transmission function at 90, 60, and 30 eV pass energies for medium area mode.

tract $n(\ln E_p/E_k)$ the offsets are removed, producing the single set of data shown in the main panel of Fig. 4. Offset removal was done by a least-squares minimization of overlapping data sets.

During this stage of the data analysis, the importance of the analyzer internal inelastic background becomes apparent. The offset removal procedure which removes sample specific information and produces the single line shown in Fig. 4 does not work at low pass energies if the internal analyzer inelastic background has not been previously removed from the data. This is because the electrons scattered inside the analyzer and the detection system dark count rate are not accounted for in Eq. (1), and must be removed from the raw spectrum before the transmission function is extracted.

Finally, by using Eq. (2) in combination with the knowledge of $n(\ln E_p/E_k)$ as obtained from the data in Fig. 4, we can calculate the transmission function for medium area mode at pass energies of 90, 60, and 30 eV. The corresponding curves are shown in Fig. 5 and, as anticipated, appear to explain the pass energy dependent structure seen in Fig. 3.

Since this spectrometer does not have a grid to electrically separate the hemispherical capacitor and the detection system, there is a pass energy dependence of the sensitivity of the detection system. Here, we have dealt with this change in sensitivity by taking it as part of the transmission function, although it is actually an artifact of the detection system and not the analyzer.

Using this same procedure, we can also study the effect on the transmission function of changing the spectrometer and source parameters (for instance, the size of the area illuminated by the source). Figure 6 contrasts the different transmission functions in medium area mode which result from the use of focused and unfocused electron beams, mimicking a change in the x-ray source spot size, as well as the closing of the iris. By varying the spot size on the sample, a large change occurs in the structure of the transmission function. This is most likely due to off-axis electrons being transmitted differently than on-axis ones. By closing down the iris, the off-axis electrons disappear from the spectrum, and we begin to see some of the features from the focused/small spot size

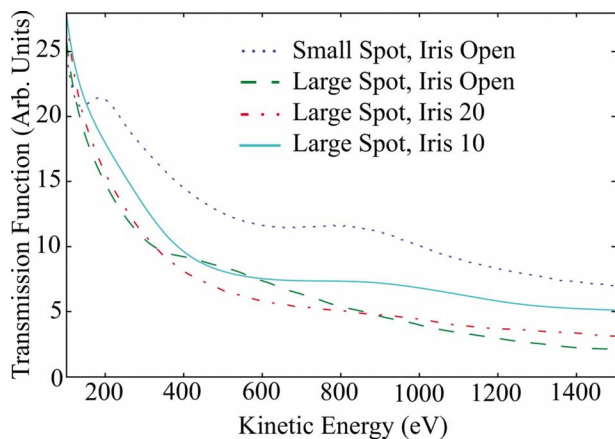


FIG. 6. (Color online) Transmission functions determined for the medium area mode with different electron spot sizes and iris settings.

spectrum reappearing (the hump at 800 eV kinetic energy, for instance). These results highlight the importance of measuring the transmission function of the spectrometer in the same configuration in which it will be operated during the experiments.

To verify that our procedure removes the transmission function, we have taken the spectra of an Au sample in a variety of modes with different transmission functions. The inset of Fig. 7 shows data taken at four different pass energies in medium area lens mode and one pass energy in medium magnification lens mode. Each spectrum has a unique transmission function. The application of our procedure for the removal of nonlinearity, inelastic scattering, and analyzer transmission returns the corrected XPS spectra shown in the main panel of Fig. 7 which are in remarkable agreement with each other. Data taken in the same lens mode at different pass energies demonstrates that the method is self-consistent (since these data are used to calculate the their own transmission function), and the data taken in different lens modes

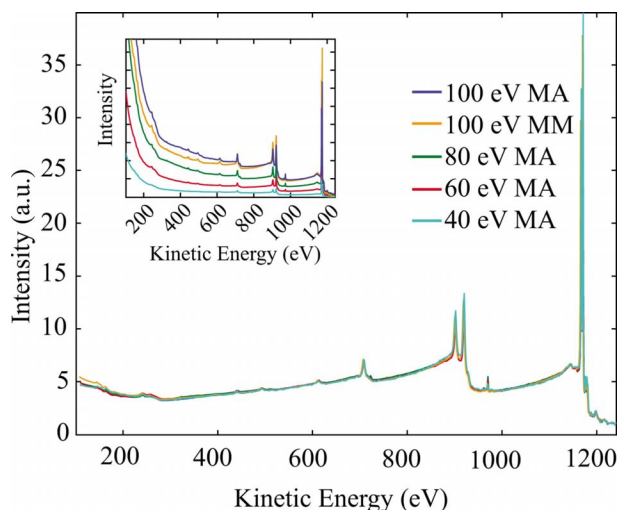


FIG. 7. (Color online) XPS spectra measured on a Au sample at different pass energies in medium area (MA) mode and medium magnification (MM) mode; the data have been corrected for analyzer nonlinearity, elastic scattering, and transmission function. The inset shows the raw data.

demonstrates that the method produces very good agreement when comparing data taken in lens modes with very different transmission characteristics.

Using this method of measuring the transmission function has the advantage of providing obvious clues when there are unaccounted spectrometer contributions to the data. For instance, the internal analyzer inelastic scattering, if left uncorrected, produces structures in the plots of $\ln I/E_p$ versus $\ln E_p/E_k$, which make it impossible to properly remove the kinetic energy dependent offsets and find the transmission function. Other spectrometer contributions with a functional dependence on E_p and E_k which is different from that of the transmission function would have a similar impact on the analysis. The ability to remove the transmission function with this method effectively indicates that, in the cases studied here, there are no other significant unaccounted for spectrometer contributions dependent on pass and kinetic energies.

Spectra taken on different materials were also found to produce equivalent transmission functions, but only when the sample size, geometry, and position were reproduced exactly between runs. This sensitivity of the transmission function to changes in sample geometry highlights the need to measure the transmission function separately for each sample that one would like to quantitatively analyze. There is no measurable change in peak position since the transmission function varies slowly across the width of a typical core level photoemission peak, so measurement of the transmission function should not be necessary for analysis based on peak positions.

VI. CONCLUSIONS

We have presented a method for characterizing the response of a hemispherical analyzer for acquiring XPS data. This involves measuring the linearity of the detection system, the strength of the analyzer internal inelastic scattering, and the transmission function of the analyzer and lens system. In our particular experimental setup, we have found that the nonlinearity of the detection system is of the order of a few percent and that contributions from the internal inelastic scattering are negligible at pass energies commonly used in XPS (accounting for less than 1% of the total intensity at 100 eV pass energy). Finally, we have measured the transmission function of the analyzer and lens system and have shown the importance of measuring the transmission function for the specific settings that will be used under operational conditions. We have also found that the presented method can be used to highlight the presence, or the lack thereof, of other pass energy and kinetic energy dependent spectrometer contributions to the measured XPS data.

ACKNOWLEDGMENTS

This work was supported by NSERC. We thank A. Damascelli for the use of his photoemission chamber; D. Fournier and J. D. F. Mottershead for providing support during the experiments; O. Schaff and S. Maehl of SPECS for suggestions on the manuscript; and M. Paul, M. Sing, and R. Claessen for initial discussions about transmission functions.

- ¹Y. M. Cross and J. E. Castle, *J. Electron Spectrosc. Relat. Phenom.* **22**, 53 (1981).
- ²P. Ruffieux, P. Schwaller, O. Groning, L. Schlapbach, P. Groning, Q. C. Herd, D. Funnemann, and J. Westermann, *Rev. Sci. Instrum.* **71**, 3634 (2000).
- ³M. P. Seah and G. C. Smith, *Surf. Interface Anal.* **17**, 855 (1991).
- ⁴M. P. Seah, *Surf. Interface Anal.* **20**, 243 (1993).
- ⁵M. P. Seah, *J. Electron Spectrosc. Relat. Phenom.* **71**, 191 (1995).
- ⁶M. P. Seah and S. J. Spencer, *J. Electron Spectrosc. Relat. Phenom.* **151**, 178 (2006).
- ⁷C. D. Wagner, L. E. Davis, M. V. Zeller, J. A. Taylor, R. H. Raymond, and L. H. Gale, *Surf. Interface Anal.* **3**, 211 (1981).
- ⁸C. S. Hemminger, T. A. Land, A. Christie, and J. C. Hemminger, *Surf. Interface Anal.* **15**, 323 (1990).
- ⁹L. T. Weng, G. Vereecke, M. J. Genet, P. Bertrand, and W. E. E. Stone, *Surf. Interface Anal.* **20**, 179 (1993).
- ¹⁰L. T. Weng, G. Vereecke, M. J. Genet, P. G. Rouxhet, J. H. Stone-Masui, P. Bertrand, and W. E. E. Stone, *Surf. Interface Anal.* **20**, 193 (1993).
- ¹¹N. Mannella, S. Marchesini, A. W. Kay, A. Nambu, T. Gresch, S. Yang, B. S. Mun, J. M. Bussat, A. Rosenhahn, and C. S. Fadley, *J. Electron Spectrosc. Relat. Phenom.* **141**, 45 (2004).
- ¹²M. Seah, I. Gilmore, and S. Spencer, *J. Electron Spectrosc. Relat. Phenom.* **120**, 93 (2001).
- ¹³J. Greenwood, M. Prutton, R. Roberts, and Z. Liu, *Surf. Interface Anal.* **20**, 891 (1993).
- ¹⁴C. Battistoni, G. Mattogno, and G. Righini, *Surf. Interface Anal.* **22**, 98 (1994).
- ¹⁵S. Hüfner, *Photoelectron Spectroscopy: Principles and Applications*, Springer Series in Solid-State Sciences 2nd ed., Vol. 82 (Springer, Berlin, 1996).
- ¹⁶D. Roy and D. Tremblay, *Rep. Prog. Phys.* **53**, 1621 (1990).